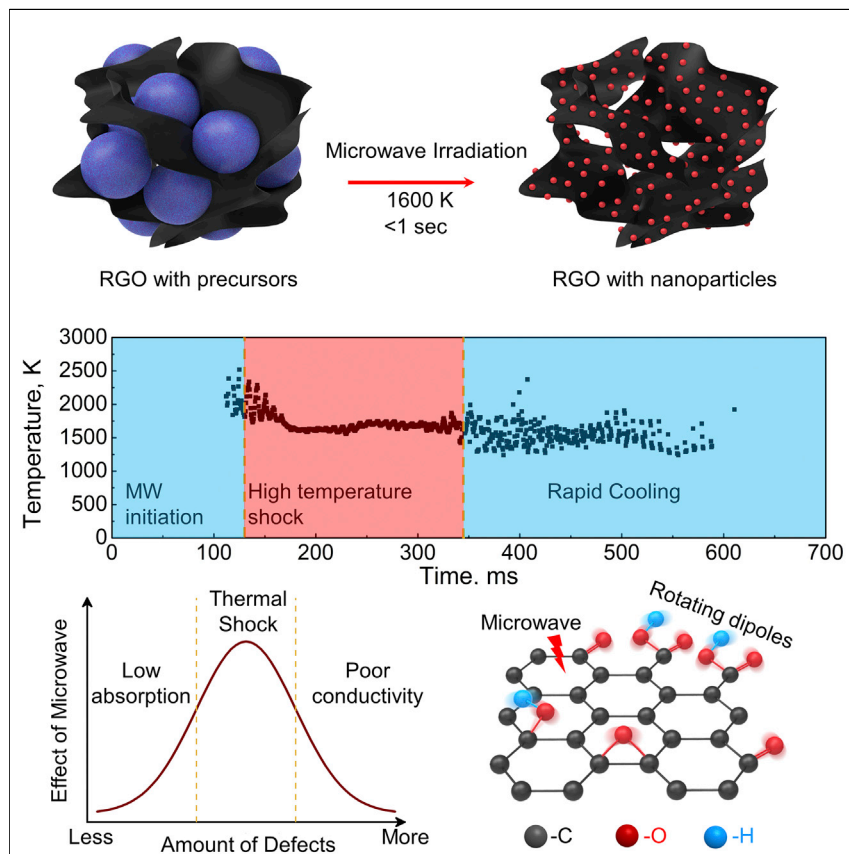


## Article

# Uniform, Scalable, High-Temperature Microwave Shock for Nanoparticle Synthesis through Defect Engineering



We demonstrate an ultrahigh-temperature thermal shock method for nanoparticle synthesis using microwave irradiation. With proper defect engineering, microwave absorption of 70% was achieved, leading to the instant temperature increase to 1,600 K in 100 ms, followed by rapid quenching to room temperature. During such extreme temperature change, the precursors are decomposed and reconstructed into nanoparticles with small size and uniform distribution. This facile, rapid, and universal synthesis technique has potential in large-scale production and suggests a new direction for nanosynthesis.

Shaomao Xu, Geng Zhong,  
Chaoji Chen, ..., Michael R.  
Zachariah, Steven M. Anlage,  
Liangbing Hu

binghu@umd.edu

## HIGHLIGHTS

A facile, rapid, and universal method for synthesis of nanoparticles

Ultrahigh temperature of 1,600 K can be achieved in less than 100 ms

The number of defects is a key parameter for achieving high temperature

A unique self-quenching mechanism for nanosynthesis is proposed



## Understanding

Dependency and conditional studies  
on material behavior

Xu et al., Matter 1, 759–769  
September 4, 2019 © 2019 Elsevier Inc.  
<https://doi.org/10.1016/j.matt.2019.05.022>



## Article

# Uniform, Scalable, High-Temperature Microwave Shock for Nanoparticle Synthesis through Defect Engineering

Shaomo Xu,<sup>1,5</sup> Geng Zhong,<sup>1,5</sup> Chaoji Chen,<sup>1,5</sup> Min Zhou,<sup>2</sup> Dylan J. Kline,<sup>3</sup> Rohit Jiji Jacob,<sup>3</sup> Hua Xie,<sup>1</sup> Shuaiming He,<sup>1</sup> Zhennan Huang,<sup>4</sup> Jiaqi Dai,<sup>1</sup> Alexandra H. Brozena,<sup>1</sup> Reza Shahbazian-Yassar,<sup>4</sup> Michael R. Zachariah,<sup>3</sup> Steven M. Anlage,<sup>2</sup> and Liangbing Hu<sup>1,6,\*</sup>

## SUMMARY

Here we demonstrate a thermal shock synthesis method triggered by microwave irradiation for the rapid synthesis of nanoparticles on reduced graphene oxide (RGO) substrate. With properly controlled reduction, RGO has high electrical conductivity while maintaining functional groups, leading to an extremely efficient microwave absorption of ~70%. The high utilization of microwaves results in the ability to raise the temperature to 1,600 K in just 100 ms, which is followed by rapid quenching to room temperature. The defects on the RGO are crucial for achieving this record-high microwave-induced temperature as these defects play a fundamental role in absorbing the radiation as well as the self-quenching mechanism. By loading precursors onto RGO, we can utilize rapid temperature change to synthesize nanoparticles. The nanoparticles are ~10 nm with uniform distribution. This facile, rapid, and universal synthesis technique has the potential to be employed in large-scale production of nanomaterials and suggests a new direction for nanosynthesis.

## INTRODUCTION

Nanoparticles are among the most widely studied nanomaterials and have been employed in various applications including catalysis,<sup>1–5</sup> photovoltaics,<sup>6–10</sup> energy storage,<sup>11–15</sup> lubricants,<sup>16,17</sup> food processing,<sup>18</sup> and drug delivery,<sup>19–23</sup> since they can drastically lower the total mass of material required while achieving the same active surface area. Wet chemistry is the most widely used method for nanoparticle synthesis due to its simplicity, inexpensive processing, and scalable nature.<sup>24,25</sup> However, nanoparticles made by wet chemistry tend to agglomerate easily, leading to a gradual loss of activity.<sup>26–28</sup> Recently, we developed a transient high-temperature pulse method for the synthesis of nanoparticles on carbon substrates and demonstrated that these materials feature superior catalytic activity and stability.<sup>29,30</sup> The key feature was the rapid heating/quenching leading to small, narrow-size distribution, unagglomerated nanoparticles. Nevertheless, with the limitation of the Joule heating procedure, it is more difficult to implement for scale-up. Thus, the focus in this work is to develop a heating method that can expand the use of the transient high-temperature pulse technique for the production of nanoparticles on a larger scale.

Microwave irradiation has been adopted as a cost-effective heating method for several decades and has been widely employed in different applications.<sup>31–33</sup> Numerous studies have employed microwave irradiation in nanoparticle synthesis,

## Progress and Potential

Despite the simplicity of conventional wet chemistry for nanosynthesis, nanoparticles fabricated by this route tend to agglomerate over the long term, particularly at high temperature and pressure, leading to a gradual loss of activity. Here we demonstrate a facile and scalable thermal shock synthesis method based on microwave irradiation for the rapid synthesis of nanoparticles on a reduced graphene oxide (RGO) substrate. Reduced at proper temperature, RGO with medium amount of defects can efficiently absorb microwaves, which leads to the rapid rise of temperature to over 1,600 K in just 100 ms. The pre-loaded precursors were easily decomposed under such high temperature and then reconstructed into nanoparticles during the subsequent rapid quenching process. Various nanoparticles were synthesized to demonstrate the feasibility and universality of this thermal shock technique. This facile, rapid, and universal synthesis method has the potential to contribute to large-scale production of nanomaterials.



but the majority of these syntheses have been conducted in liquids, which share many of the same pitfalls as conventional wet chemistry.<sup>34–41</sup> Carbon substrates and polymers have been used as microwave absorber to enable microwave syntheses of nanomaterials under solid-state conditions.<sup>42–50</sup> These techniques often require relatively long heating times (>1 min) and the peak temperatures tend to be relatively low (<1,000°C). As a result, precursor materials do not undergo ultrafast melting or reconstruction, causing the resulting particles to suffer from the aforementioned disadvantages often associated with wet chemical processes.

In this work, we develop a rapid thermal shock method for nanoparticle synthesis using microwave irradiation. Reduced graphene oxide (RGO) has been demonstrated as an excellent carbon support for nanoparticles and an efficient microwave absorber.<sup>51–53</sup> Using RGO produced under controlled reduction conditions, we demonstrate that its temperature can be raised to over 1,600 K in just 100 ms by the absorption of microwave radiation—a temperature that is over 2-fold higher than in previously reported microwave synthesis methods.<sup>40–43</sup> Moreover, at these high temperatures the kinetics become sufficiently fast such that reaction times are less than 1 s. This is dramatically shorter than any reported in previous studies using microwave synthesis.<sup>41–44</sup> By loading precursor materials onto the RGO, the rapid temperature increase upon microwaving causes the precursors to undergo decomposition, and the subsequent rapid cooling leads to particle nucleation. Due to this ultrafast phase transition, the resulting nanoparticles are both small in size (~10 nm) and feature a uniform size distribution. The rapid quench also freezes any mobility, preventing agglomeration. We also show that the defect concentration in the RGO substrate is a key factor in successfully triggering this thermal shock effect, as the defects aid in the microwave absorption as well as participate in the rapid self-quenching mechanism. Additionally, with the simplicity of microwave heating process, the synthesis can be easily scaled up while maintaining the uniformity of the nanoparticle size. This scalable, high-temperature pulse generated by microwave irradiation provides a new route for the synthesis of uniform nanoparticles and can shed light on further innovation in nanosynthesis.

## RESULTS AND DISCUSSION

Figure 1 illustrates the concept of this scalable thermal shock synthesis using microwave irradiation. Since the microwave is uniformly distributed in a large space, the synthesis can be easily scaled up to produce large batches of powder RGO samples decorated with nanoparticles. Initially, we loaded the RGO with salt precursors that are microscale in size (schematics in Figure 1A). After less than 1 s of microwave irradiation, during which the temperature was as high as 1,600 K, the micron-sized precursors decompose, and upon quenching nucleate to form nanoparticles decorating the RGO film. Although there was no apparent macroscopic change before and after microwave heating (photos in Figure 1A), the nanoscale morphology is drastically different. We have found that the rapid temperature change can only be achieved by carefully controlling the defect density on the RGO substrate (Figure 1B). Sufficient defects are needed first to promote high microwave absorption efficiency; however, too high a defect density leads to poor thermal conductivity and inhomogeneous sample temperature. Compared with previous studies, the microwave irradiation synthesis method reported in this work has the highest temperature and the shortest heating time (Figure 1C), making it a unique thermal shock process.

To demonstrate the feasibility of the thermal shock synthesis using microwave irradiation, we chose to synthesize cobalt sulfide (CoS) nanoparticles as a proof of

<sup>1</sup>Department of Materials Science and Engineering, University of Maryland, College Park, MD 20742, USA

<sup>2</sup>Department of Physics, Center for Nanophysics and Advanced Materials, University of Maryland, College Park, MD 20742, USA

<sup>3</sup>Department of Chemistry, University of Maryland, College Park, MD 20742, USA

<sup>4</sup>Department of Mechanical & Industrial Engineering, University of Illinois at Chicago, Chicago, IL 60607, USA

<sup>5</sup>These authors contributed equally

<sup>6</sup>Lead Contact

\*Correspondence: binghu@umd.edu

<https://doi.org/10.1016/j.matt.2019.05.022>

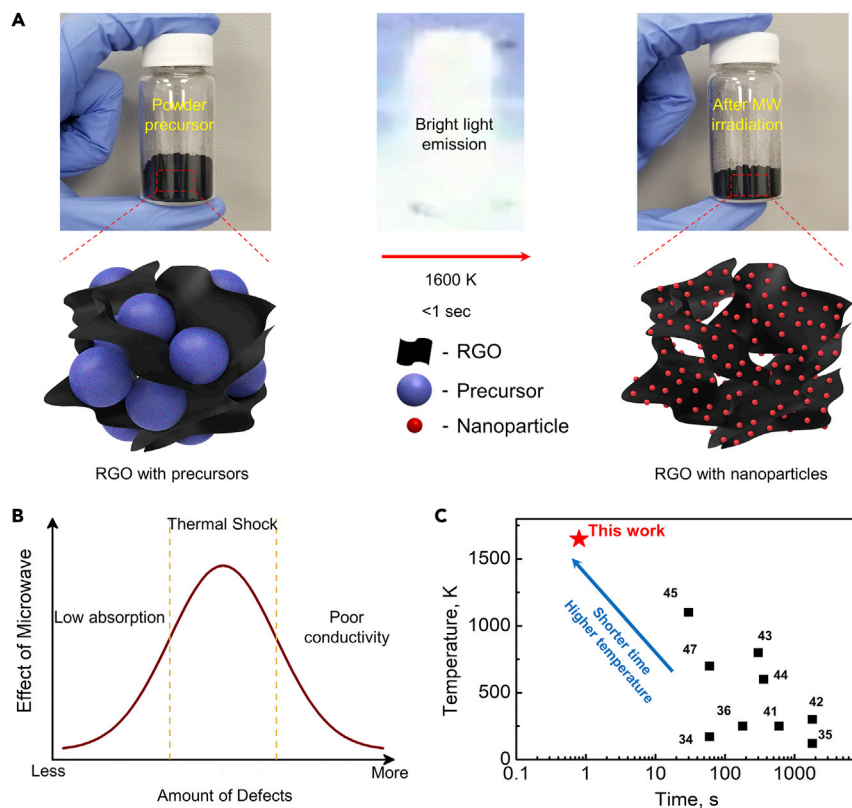


**Figure 1. Schematic of the Thermal Shock Method Using Microwave Irradiation for Nanoparticle Synthesis**

(A) Photos and schematics of the RGO loaded with precursor before (left) and after microwave (MW) irradiation (right), respectively. After microwave irradiation, the RGO is decorated with uniformly distributed nanoparticles.

(B) The effect of defects on the thermal shock effect, showing that the thermal shock effect only occurs when there is both good microwave absorption and good thermal conduction.

(C) Comparison of heating time and temperature between this work and previous studies using microwave irradiation, demonstrating the massively shorter reaction time and higher heating temperature of our technique.

concept. Figure 2A shows the photographs of the RGO sample during the process of microwave irradiation, captured using a high-speed video camera. The images are computer processed to capture the raw color of each pixel and enabling a spatial-and time-resolved ratio pyrometer to obtain the temperature (Figure S1). Figure 2B shows a plot of the sample light emission intensity versus time over the synthesis. By fitting the light emission to Planck's law for gray-body radiation, we were able to calculate the average temperature over all pixels (Figure 2C). Visible emission is observed approximately ~100 ms after the microwave is turned on and once several bright spots can be seen. These hotspots are localized so that the total emission is relatively low (Figure 2B); nevertheless, the average temperature at ~100 ms was as high as 2,000 K (Figure 2C). As the heating progressed, the initial locally generated heat spreads to the whole sample, leading to the rapid increase in light intensity, making the sample very bright. Although the light emission becomes stronger, since the whole sample is hot the temperature drops and stabilizes at ~1,600 K. After ~250 ms of microwave heating, the sample emits light with peak brightness. Thereafter, the light intensity starts dropping and the sample becomes visibly dimmer, until it eventually extinguishes after 600 ms and we cannot measure

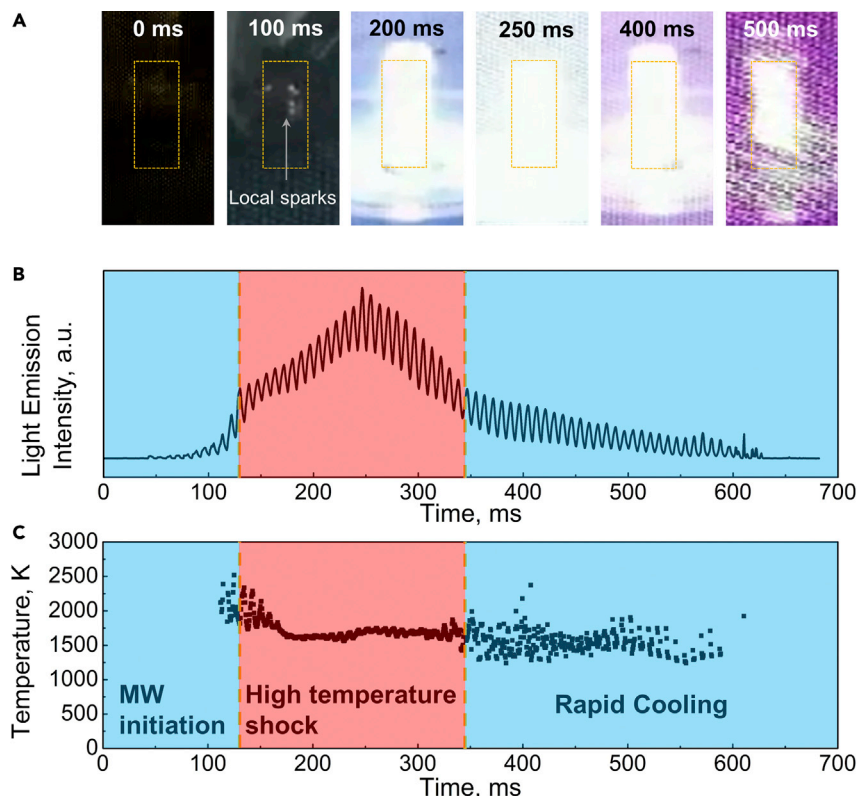


**Figure 2. Analysis of the Thermal Shock Process**

(A) Photos of RGO sample during thermal shock process: before microwave, and 100, 200, 250, 400, and 500 ms after turning on the microwave irradiation.

(B) The intensity of light emission during the thermal shock. The dashed boxes indicate the position of the sample in the photo.

(C) Profile of average temperature captured during the microwave (MW) thermal shock made by fitting the gray-body theory to the intensity of light emission of captured pixels.

temperature past this point. The total effective heating time of ~600 ms is orders of magnitude shorter than that of previous reports,<sup>41–44</sup> making this a unique thermal shock process. Although the intensity of the light emission changes constantly during the microwave synthesis (Figure 2B), the temperature is almost constant during the whole heating process, maintaining a high temperature of ~1,600 K (Figure 2C). The temperature reported in Figure 2C is the median temperature spatially averaged over the entire sample. As such the temperature is biased toward the hotspots that emit the most light. This is the reason why the emission entity can increase while the temperature appears to be constant. Based on these results, we divide the microwave synthesis into three periods: (1) initial heating; (2) high-temperature thermal shock; and (3) rapid cooling.

We employed scanning and transmission electron microscopy (SEM and TEM) to study the morphology of the nanoparticle products (Figure 3). Lower-magnification SEM (Figure 3A) and TEM (Figure S2) capture the panorama of the synthesized product, which shows that the CoS nanoparticles feature a uniform size distribution ( $10.8 \pm 2.3$  nm, Figure 3B) that densely covers the surface of the RGO. High-magnification TEM images indicate that the nanoparticles are 8–10 nm in diameter with lattice spacing of 0.19 nm, which corresponds to the (102) plane of CoS (Figure 3C). X-ray diffraction was employed to study the crystal structure of the product, which

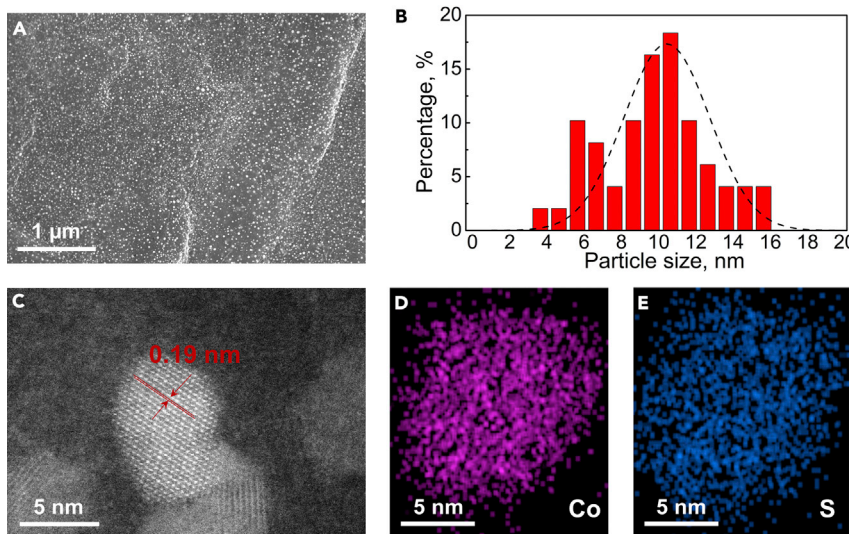


**Figure 3. Characterization of the CoS Nanoparticles Synthesized by Thermal Shock Using Microwave Irradiation**

(A) SEM image of the CoS nanoparticles on RGO synthesized by microwave-induced thermal shock. (B) Size distribution of the CoS nanoparticles, which have an average size of  $10.8 \pm 2.3$  nm. (C) High-magnification TEM image indicating a lattice space of 0.19 nm, corresponding to the (102) plane of CoS. (D and E) Elemental mapping of the (D) Co and (E) S of the CoS nanoparticles, revealing the almost identical distribution of Co and S.

shows the characteristic peaks of CoS (Figure S3). Energy dispersive X-ray spectroscopy mapping shows the matching between the distribution of Co (Figure 3D) and S (Figure 3E), indicating that the expected product composition was achieved.

Due to their small size and uniform distribution, the CoS nanoparticles show excellent catalytic performance toward the hydrogen evolution reaction (HER) (Figure S4). In acidic solution, the CoS nanoparticles show a low onset overpotential of 120 mV (Figure S4A) and a Tafel slope of 102 mV/dec (Figure S4B), indicating the remarkable catalytic activity of the material. Additionally, the overpotential only showed a shift of 20 mV after 1,000 HER cycles (Figure S4C), demonstrating the excellent stability of the nanoparticles for long-term operation. At an overpotential of 180 mV, the current density remains almost unchanged for over 10 h, which indicates the catalyst's ability to survive high-stress production (Figure S4D). This superb activity and remarkable stability prove that our thermal shock synthesis using microwave irradiation is an excellent choice for the fabrication of nanocatalysts.

Since this method using microwave irradiation should be easily applied for large-scale production, the uniformity of the synthesized nanoparticles in large batches is a crucial criterion for judging the technique's feasibility. To study the uniformity of the synthesis, we synthesized 100 mg of CoS/RGO samples in a single thermal shock process (Figure S5). From this batch, we imaged the material at five different positions using SEM to compare the nanomaterial morphology and distribution. Even at these different locales, the morphologies remained almost identical, with all five samples showing ~10-nm-sized CoS nanoparticles densely decorating the surface of the RGO. These results show that thermal shock microwave heating is an exceptional choice for the scaled-up synthesis of small and uniform nanoparticles.

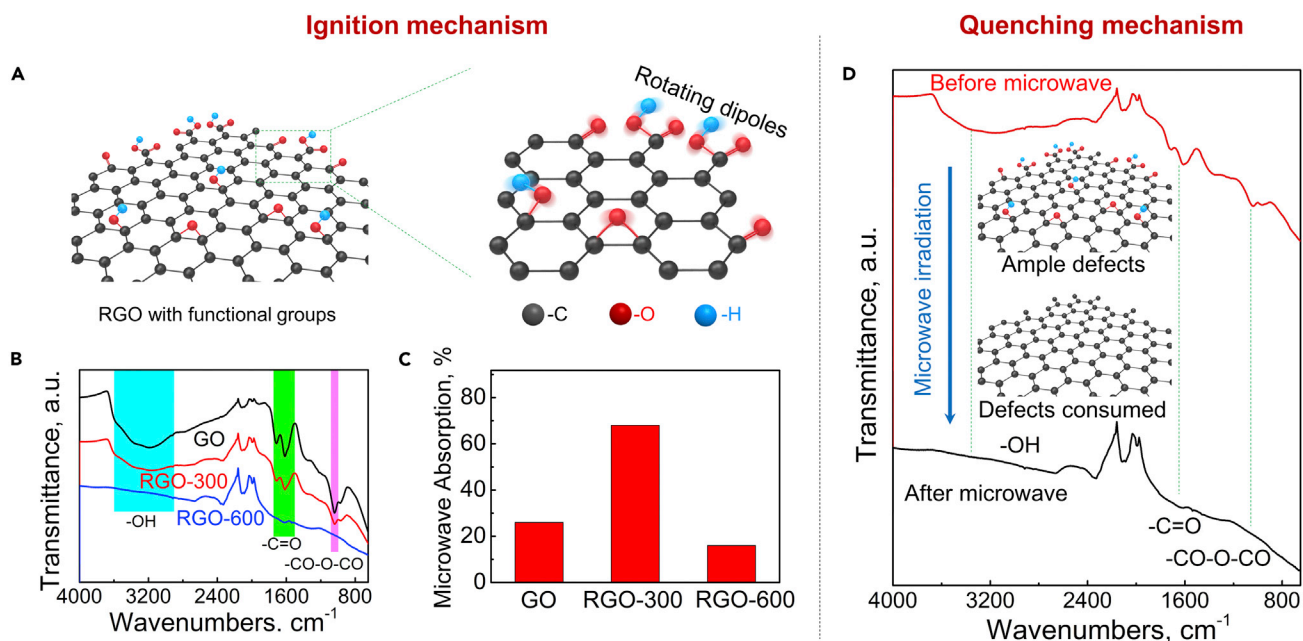


**Figure 4. Mechanism of the Thermal Shock Induced by Microwave Irradiation**

(A) RGO film with numerous functional groups before microwave irradiation. A magnified view depicts the rotating dipole of the RGO functional groups during microwave irradiation.

(B) FTIR of GO, RGO-300, and RGO-600, showing the low content of functional groups of RGO-600.

(C) Comparison of microwave absorption between GO, RGO-300, and RGO-600. Only RGO-300 demonstrates a high microwave absorption of ~70%. (D) FTIR of RGO-300 before and after microwave treatment, indicating the consumption of functional groups during the microwave synthesis. The inset schematics show the difference in the defect content of the RGO-300 before and after the microwave synthesis.

To understand the mechanism of the thermal shock induced by microwave irradiation, we tested different RGO substrates made at different reducing temperatures. Our results showed that only RGO reduced at 300°C (RGO-300) demonstrated the thermal shock phenomenon, while pristine GO (GO) and RGO reduced at 600°C (RGO-600) did not trigger such behavior. We hypothesize that this is due to the difference in the amount of defects and functional groups between RGO with various degrees of reduction. RGO is rich in various oxygen defects and functional groups (Figure 4A). The dipoles of these functional groups can rotate in the presence of an electromagnetic field, thus leading to frictional heating, which we believe is the main contributor to the microwave absorption. The oxygen-rich functional groups rapidly absorb the microwaves to generate heat and drastically increase the sample temperature. Another mechanism of microwave absorption involves the generation of eddy currents, which is induced when a conductive material is treated with an oscillating electromagnetic field. Due to the conducting nature of RGO, an eddy current loop can be formed when placed in a microwave field, leading to Joule heating and triggering the thermal shock. Additionally, in order to trigger this thermal shock effect, high thermal conductivity is also required to transport the absorbed heat to the whole sample. Therefore, the RGO substrate needs to meet three requirements to maximize the ability to trigger the thermal shock synthesis. (1) The substrate should have an adequate number of functional groups after reduction to provide sufficient rotating dipoles in the microwave field. (2) The substrate should have sufficient electronic conductivity to generate eddy currents in the presence of microwaves. However, the conductivity should not be so high that the substrate is almost metallic, leading to the majority of the microwaves being reflected instead of absorbed. (3) High thermal conductivity is also a prerequisite for the thermal shock

effect, since the absorbed heat needs to quickly spread through the whole sample. Therefore, the degree of the RGO reduction is a crucial factor for this method of nanoparticle synthesis.

To better understand the effect of defects and functional groups, we employed Fourier transform infrared spectroscopy (FTIR) (Figure 4B) to study different substrates. The results revealed that RGO-600 has a lower content of –OH, –C=O, and –CO–O–CO groups compared with GO and RGO-300. The low functional group content combined with the almost metallic properties of RGO-600, leads to a low microwave absorption of only 20% (Figure 4C), which explains the absence of the thermal shock phenomenon with the RGO-600 substrate. On the other hand, because RGO-300 has moderate electronic conductivity to generate eddy currents and sufficient functional groups to produce rotating dipoles, it has a high microwave absorption of over 60%, leading to its strong ability to trigger the thermal shock. It is worth noting that GO does not trigger the thermal shock either, despite its high content of functional groups, likely because its low electronic conductivity leads to the inability to form eddy current loops and thus absorb less microwave radiation. Additionally, due to the low thermal conductivity of GO, even though microwaves can be absorbed and areas of the sample can become heated, the heat is isolated and cannot easily spread to the whole sample, leading to the failure of the overall thermal shock effect. The combination of high functional group content, microwave absorption, and thermal conductivity results in RGO-300 being the best substrate for this application.

After the microwave synthesis in argon, the FTIR spectrum reveals drastically lower content of –OH, –C=O, and –CO–O–CO groups (Figure 4D), indicating the consumption of the functional groups and a more graphitic structure. As a result, the substrate's ability to absorb microwave radiation is significantly attenuated, creating a self-quenching process that results in a rapid decrease in temperature (Figure 4D). This whole synthesis process occurs in just 600 ms. In summary, the electronic conductivity and functional groups enable the absorption of microwave irradiation and the initial isolated heating effect, which is followed by the conduction of heat to the whole sample. This process ultimately consumes the substrate functional groups, causing the temperature to immediately drop due to the loss of microwave absorption.

The feasibility of the thermal shock synthesis using microwave irradiation is not limited to just the synthesis of CoS nanoparticles. We demonstrated the universality of this method by synthesizing other materials, including ruthenium (Ru), palladium (Pd), and iridium (Ir) nanoparticles (Figures 5 and S7). As a result of the high scalability of the microwave synthesis, we were able to produce over 100 mg of product in a single batch synthesis (Figures 5A–5C). After synthesis, the nanoparticles formed on the RGO film featured a uniform size of ~20 nm (Figures 5D–5F). Single nanoparticle microanalysis shows lattice spacings of 0.2 nm (Ru), 0.22 nm (Pd), and 0.22 nm (Ir), corresponding to the (111) plane of zero-valent metals. This successful synthesis of metal nanoparticles demonstrates the universality of the thermal shock synthesis technique by microwave irradiation. The rapid and facile approach can be further employed in the synthesis of other various nanomaterials.

### Conclusion

In conclusion, we have developed a facile and scalable thermal shock method for nanoparticle synthesis using microwave irradiation. Using RGO reduced at 300°C as the microwave absorber, this substrate's ample functional groups lead to high microwave absorption and consequently a rapid local temperature increase to

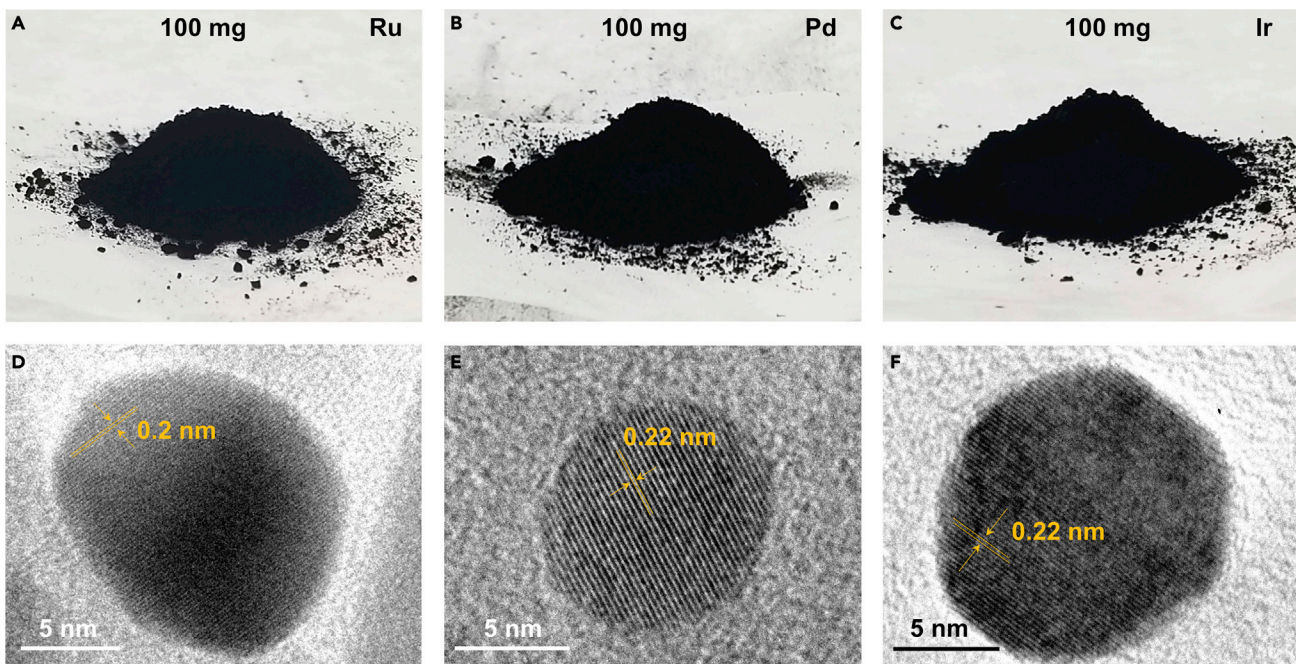


**Figure 5. Universality of the Thermal Shock Synthesis Induced by Microwave Irradiation**

(A–C) Photos of the bulk samples of the (A) Ru, (B) Pd, and (C) Ir nanoparticles on RGO, respectively. (D–F) High-magnification TEM image of individual (D) Ru, (E) Pd, and (F) Ir nanoparticles.

over 2,000 K in just 100 ms. The heat then spreads over the entire sample due to the good thermal conductivity of RGO, which results in a stabilized heating temperature of 1,600 K. After the consumption of the functional groups, the temperature rapidly drops in less than 300 ms, resulting in a unique self-quenching mechanism. Such rapid and extreme temperature change leads to ultrafast melting and decomposition of loaded precursor materials and their subsequent condensation into nanoparticles, which are both uniformly small ( $\sim 10$  nm) and unagglomerated. Using CoS as a proof of concept, the synthesized nanoparticles densely decorate the surface of the RGO, which leads to excellent catalytic activity for HER performance. Additionally, due to the simplicity of the microwave irradiation treatment, the synthesis can be scaled up to large batch synthesis, the uniformity of which we have proved through the identical morphology of the products at different locations of the batch material. This thermal shock nanoparticle synthesis using microwave irradiation can also be applied to other materials. The rapid, facile, and scalable thermal shock method made possible by microwave heating and an electrically and thermally conductive substrate is advantageous over conventional wet chemistry techniques and has the potential to be employed for large-scale nanoparticle production.

## EXPERIMENTAL PROCEDURES

### Synthesis of Nanoparticles

All chemicals were purchased from Sigma-Aldrich. For synthesis of the CoS nanoparticles, 10 mg of cobalt acetate tetrahydrate and 15 mg of thiourea were dissolved in 10 mL of deionized water. The resulting solution was then mixed with 2 mL of 4 mg/mL GO solution, which was synthesized by a modified Hummer's method. The solution was then sealed and sonicated for 1 h before casting onto a glass slide. After the water evaporated, the resulting film was scraped off the glass slide into a relatively fine powder. After a 1-h pre-reduction at 300°C in argon atmosphere, the powder was sealed in an argon-filled glovebox and directly transferred into a

microwave oven (Panasonic, 1,200 W) for irradiation treatment. A similar synthesis was employed for the fabrication of the Ru, Pd, and Ir nanoparticles, with ruthenium chloride, palladium chloride, and iridium chloride as the respective precursors. The precursor-GO mixture was achieved by mixing 10 mL of precursor solution (1 mg/mL) and 2 mL of GO solution (4 mg/mL).

### Materials Characterization

SEM and TEM images were captured with a Hitachi SU-70 FEG scanning electron microscope and a JEM 2100 FEG transmission electron microscope, respectively. The FTIR spectra were measured using a Thermo Nicolet NEXUS 670 FTIR spectrometer.

Details of temperature measurements, electrochemical measurements, and microwave absorption measurements can be found in [Supplemental Information](#).

### SUPPLEMENTAL INFORMATION

Supplemental Information can be found online at <https://doi.org/10.1016/j.matt.2019.05.022>.

### ACKNOWLEDGMENTS

L.H. acknowledges the financial support from the Dean's office of Department of Materials Science and Engineering for the equipment setup. We acknowledge the support of the Maryland NanoCenter and its AIMLab. M.Z. and S.M.A. are supported by the DOE under award #DE-SC0018788.

### AUTHOR CONTRIBUTIONS

L.H. and S.X. designed the project. G.Z. and S.X. synthesized the materials. C.C., G.Z., and S.X. analyzed the data. G.Z., S.H., H.X., and J.D. contributed to the materials characterization. S.X. tested the electrochemical performance. M.R.Z., R.J.J., and D.J.K. did the temperature measurements. M.Z. and S.M.A. performed microwave absorption measurements. Z.H. and R.S.-Y. contributed to the high-resolution TEM analyses. L.H., G.Z., S.X., C.C., and A.H.B. wrote the paper. All authors contributed to commenting on the final manuscript.

### DECLARATION OF INTERESTS

An invention disclosure (PS-2019-037) has been filed with office of technology commercialization at University of Maryland, with L.H., S.X., and G.Z. as inventors, covering the high-temperature microwave processing method described herein. The authors declare no competing interests.

Received: January 30, 2019

Revised: April 5, 2019

Accepted: May 20, 2019

Published: August 28, 2019

### REFERENCES

1. Liu, L., and Corma, A. (2018). Metal catalysts for heterogeneous catalysis: from single atoms to nanoclusters and nanoparticles. *Chem. Rev.* 118, 4981–5079.
2. Zhou, Y., Jin, C., Li, Y., and Shen, W. (2018). Dynamic behavior of metal nanoparticles for catalysis. *Nano Today* 20, 101–120.
3. Biffis, A., Centomo, P., Del Zotto, A., and Zecca, M. (2018). Pd metal catalysts for cross-couplings and related reactions in the 21st century: a critical review. *Chem. Rev.* 118, 2249–2295.
4. Li, Z., and Xu, Q. (2017). Metal-nanoparticle-catalyzed hydrogen generation from formic acid. *Acc. Chem. Res.* 50, 1449–1458.
5. Gewirth, A.A., Varnli, J.A., and DiAscro, A.M. (2018). Nonprecious metal catalysts for oxygen reduction in heterogeneous aqueous systems. *Chem. Rev.* 118, 2313–2339.
6. Hasobe, T., Imahori, H., Kamat, P.V., Ahn, T.K., Kim, S.K., Kim, D., Fujimoto, A., Hirakawa, T., and Fukuzumi, S. (2005). Photovoltaic cells using composite nanoclusters of porphyrins

- and fullerenes with gold nanoparticles. *J. Am. Chem. Soc.* 127, 1216–1228.
7. Ma, W., Luther, J.M., Zheng, H., Wu, Y., and Alivisatos, A.P. (2009). Photovoltaic devices employing ternary  $Pb_xSe_{1-x}$  nanocrystals. *Nano Lett.* 9, 1699–1703.
8. Liang, Z., Dzienis, K.L., Xu, J., and Wang, Q. (2006). Covalent layer-by-layer assembly of conjugated polymers and CdSe nanoparticles: multilayer structure and photovoltaic properties. *Adv. Funct. Mater.* 16, 542–548.
9. Paci, B., Spyropoulos, G.D., Generosi, A., Bailo, D., Albertini, V.R., Stratikis, E., and Kymakis, E. (2011). Enhanced structural stability and performance durability of bulk heterojunction photovoltaic devices incorporating metallic nanoparticles. *Adv. Funct. Mater.* 21, 3573–3582.
10. Beek, W.J.E., Wienk, M.M., and Janssen, R.A.J. (2004). Efficient hybrid solar cells from zinc oxide nanoparticles and a conjugated polymer. *Adv. Mater.* 16, 1009–1013.
11. Shelke, M.V., Gullapalli, H., Kalaga, K., Rodrigues, M.-T.F., Devarapalli, R.R., Vajtai, R., and Ajayan, P.M. (2017). Facile synthesis of 3D anode assembly with Si nanoparticles sealed in highly pure few layer graphene deposited on porous current collector for long life Li-ion battery. *Adv. Mater.* 4, 1601043.
12. Yang, S., Qiao, Y., He, P., Liu, Y., Cheng, Z., Zhu, J., and Zhou, H. (2017). A reversible lithium–CO<sub>2</sub> battery with Ru nanoparticles as a cathode catalyst. *Energy Environ. Sci.* 10, 972–978.
13. Tabassum, H., Zou, R., Mahmood, A., Liang, Z., Wang, Q., Zhang, H., Gao, S., Qu, C., Guo, W., and Guo, S. (2018). A universal strategy for hollow metal oxide nanoparticles encapsulated into B/N co-doped graphitic nanotubes as high-performance lithium-ion battery anodes. *Adv. Mater.* 30, 1705441.
14. Chang, W.-C., Tseng, K.-W., and Tuan, H.-Y. (2017). Solution synthesis of iodine-doped red phosphorus nanoparticles for lithium-ion battery anodes. *Nano Lett.* 17, 1240–1247.
15. Xia, G., Gao, Q., Sun, D., and Yu, X. (2017). Porous carbon nanofibers encapsulated with peapod-like hematite nanoparticles for high-rate and long-life battery anodes. *Small* 13, 1701561.
16. Rapoport, L., Fleischer, N., and Tenne, R. (2003). Fullerene-like WS<sub>2</sub> nanoparticles: superior lubricants for harsh conditions. *Adv. Mater.* 15, 651–655.
17. Tevet, O., Von-Huth, P., Popovitz-Biro, R., Rosentsveig, R., Wagner, H.D., and Tenne, R. (2011). Friction mechanism of individual multilayered nanoparticles. *Proc. Natl. Acad. Sci. U.S.A.* 108, 19901–19906.
18. Chaudhry, Q., Scotter, M., Blackburn, J., Ross, B., Boxall, A., Castle, L., Aitken, R., and Watkins, R. (2008). Applications and implications of nanotechnologies for the food sector. *Food Addit. Contam. Part A* 25, 241–258.
19. Arrebo, M., Fernandez-Pacheco, R., Ibarra, M.R., and Santamaría, J. (2007). Magnetic nanoparticles for drug delivery. *Nano Today* 2, 22–32.
20. Liang, M., Lu, J., Kovochich, M., Xia, T., Ruehm, S.G., Nel, A.E., Tamano, F., and Zink, J.I. (2008). Multifunctional inorganic nanoparticles for imaging, targeting, and drug delivery. *ACS Nano* 2, 889–896.
21. Kim, J., Kim, H.S., Lee, N., Kim, T., Kim, H., Yu, T., Song, I.C., Moon, W.K., and Hyeon, T. (2008). Multifunctional uniform nanoparticles composed of a magnetite nanocrystal core and a mesoporous silica shell for magnetic resonance and fluorescence imaging and for drug delivery. *Angew. Chem. Int. Ed.* 47, 8438–8441.
22. Tang, F., Li, L., and Chen, D. (2012). Mesoporous silica nanoparticles: synthesis, biocompatibility and drug delivery. *Adv. Mater.* 24, 1504–1534.
23. Slowing, I.I., Trewyn, B.G., Giri, S., and Lin, V.S.-Y. (2007). Mesoporous silica nanoparticles for drug delivery and biosensing applications. *Adv. Funct. Mater.* 17, 1225–1236.
24. Zhang, P., Shao, C., Zhang, Z., Zhang, M., Mu, J., Guo, Z., and Liu, Y. (2011). In situ assembly of well-dispersed Ag nanoparticles (AgNPs) on electrospun carbon nanofibers (CNFs) for catalytic reduction of 4-nitrophenol. *Nanoscale* 3, 3357–3363.
25. Liu, L., Gao, F., Concepción, P., and Corma, A. (2017). A new strategy to transform mono and bimetallic non-noble metal nanoparticles into highly active and chemoselective hydrogenation catalysts. *J. Catal.* 350, 218–225.
26. Jin, Z., Nackashi, D., Lu, W., Kittrell, C., and Tour, J.M. (2010). Decoration, migration, and aggregation of palladium nanoparticles on graphene sheets. *Chem. Mater.* 22, 5695–5699.
27. Chen, Y., Li, C.W., and Kanan, M.W. (2012). Aqueous CO<sub>2</sub> reduction at very low overpotential on oxide-derived au nanoparticles. *J. Am. Chem. Soc.* 134, 19969–19972.
28. Chung, D.Y., Jun, S.W., Yoon, G., Kwon, S.G., Shin, D.Y., Seo, P., Yoo, J.M., Shin, H., Chung, Y.-H., Kim, H., et al. (2015). Highly durable and active PtFe nanocatalyst for electrochemical oxygen reduction reaction. *J. Am. Chem. Soc.* 137, 15478–15485.
29. Yao, Y., Huang, Z., Xie, P., Lacey, S.D., Jacob, R.J., Xie, H., Chen, F., Nie, A., Pu, T., Rehwoldt, M., et al. (2018). Carbothermal shock synthesis of high-entropy-alloy nanoparticles. *Science* 359, 1489–1494.
30. Li, T., Pickel, A.D., Yao, Y., Chen, Y., Zeng, Y., Lacey, S.D., Li, Y., Wang, Y., Dai, J., Wang, Y., et al. (2018). Thermoelectric properties and performance of flexible reduced graphene oxide films up to 3,000 K. *Nat. Energy* 3, 148–156.
31. Jones, D.A., Lelyveld, T.P., Mavrofidis, S.D., Kingman, S.W., and Miles, N.J. (2002). Microwave heating applications in environmental engineering—a review. *Resour. Conserv. Recycl.* 34, 75–90.
32. Faraji, S., and Ani, F.N. (2014). Microwave-assisted synthesis of metal oxide/hydroxide composite electrodes for high power supercapacitors—a review. *J. Power Sources* 263, 338–360.
33. Roy, R., Agrawal, D., Cheng, J., and Gedevanishvili, S. (1999). Full sintering of powdered-metal bodies in a microwave field. *Nature* 399, 668–670.
34. Liu, Z., Guo, B., Hong, L., and Lim, T.H. (2006). Microwave heated polyol synthesis of carbon-supported PtSn nanoparticles for methanol electrooxidation. *Electrochim. Commun.* 8, 83–90.
35. Bilecka, I., Elser, P., and Niederberger, M. (2009). Kinetic and thermodynamic aspects in the microwave-assisted synthesis of ZnO nanoparticles in benzyl alcohol. *ACS Nano* 3, 467–477.
36. Vollmer, C., Redel, E., Abu-Shandi, K., Thomann, R., Manyar, H., Hardacre, C., and Janiak, C. (2010). Microwave irradiation for the facile synthesis of transition-metal nanoparticles (NPs) in ionic liquids (ILs) from metal-carbonyl precursors and Ru-, Rh-, and Ir-NP/IL dispersions as biphasic liquid-liquid hydrogenation nanocatalysts for cyclohexene. *Chem. Eur. J.* 16, 3849–3858.
37. Fuku, K., Hayashi, R., Takakura, S., Kamegawa, T., Mori, K., and Yamashita, H. (2013). The synthesis of size- and color-controlled silver nanoparticles by using microwave heating and their enhanced catalytic activity by localized surface plasmon resonance. *Angew. Chem. Int. Ed.* 52, 7446–7450.
38. Liao, X., Zhu, J., Zhong, W., and Chen, H.-Y. (2001). Synthesis of amorphous Fe<sub>2</sub>O<sub>3</sub> nanoparticles by microwave irradiation. *Mater. Lett.* 50, 341–346.
39. Hu, Y., Liu, Y., Qian, H., Li, Z., and Chen, J. (2010). Coating colloidal carbon spheres with CdS nanoparticles: microwave-assisted synthesis and enhanced photocatalytic activity. *Langmuir* 36, 18570–18575.
40. Tsuji, M., Hashimoto, M., Nishizawa, Y., Kubokawa, M., and Tsuji, T. (2005). Microwave-assisted synthesis of metallic nanostructures in solution. *Chem. Eur. J.* 11, 440–452.
41. Hu, H., Yang, H., Huang, P., Cui, D., Peng, Y., Zhang, J., Lu, F., Lian, J., and Shi, D. (2010). Unique role of ionic liquid in microwave-assisted synthesis of monodisperse magnetite nanoparticles. *Chem. Commun. (Camb.)* 46, 3866–3868.
42. Lin, Y., Baggett, D.W., Kim, J.-W., Siochi, E.J., and Connell, J.W. (2011). Instantaneous formation of metal and metal oxide nanoparticles on carbon nanotubes and graphene via solvent-free microwave heating. *ACS Appl. Mater. Interfaces* 3, 1652–1664.
43. Zhang, X., and Manohar, S.K. (2006). Microwave synthesis of nanocarbons from conducting polymers. *Chem. Commun. (Camb.)* 0, 2477–2479.
44. Liu, Z., Zhang, X., Poyraz, S., Surwade, S.P., and Manohar, S.K. (2010). Oxidative template for conducting polymer nanoclips. *J. Am. Chem. Soc.* 132, 13158–13159.
45. Liu, Z., Wang, J., Kushvaha, V., Poyraz, S., Tippur, H., Park, S., Kim, M., Liu, Y., Bar, J., Chen, H., and Zhang, X. (2011). Poptube approach for ultrafast carbon nanotube growth. *Chem. Commun. (Camb.)* 47, 9912–9914.

46. Poyraz, S., Zhang, L., Schroder, A., and Zhang, X. (2015). Ultrafast microwave welding/reinforcing approach at the interface of thermoplastic materials. *ACS Appl. Mater. Interfaces* 7, 22469–22477.
47. Liu, Z., Zhang, L., Wang, R., Poyraz, S., Cook, J., Bozack, M.J., Das, S., Zhang, X., and Hu, L. (2016). Ultrafast microwave nano-manufacturing of fullerene-like metal chalcogenides. *Sci. Rep.* 6, 22503.
48. Bi, Y., Nautiyal, A., Zhang, H., Luo, J., and Zhang, X. (2018). One-pot microwave synthesis of NiO/MnO<sub>2</sub> composite as a high-performance electrode material for supercapacitors. *Electrochim. Acta* 260, 952–958.
49. Tian, Y., Yang, X., Nautiyal, A., Zheng, Y., Guo, Q., Luo, J., and Zhang, X. (2019). One-step microwave synthesis of MoS<sub>2</sub>/MoO<sub>3</sub>@graphite nanocomposite as an excellent electrode material for supercapacitors. *Adv. Compos. Hybrid Mater.* 2, 151–161.
50. Liu, Y., Zhang, X., Poyraz, S., Zhang, C., and Xin, J.H. (2018). One-step synthesis of multifunctional zinc-iron-oxide hybrid carbon nanowires by chemical fusion for supercapacitors and interfacial water marbles. *ChemNanoMat* 4, 546–556.
51. Xu, S., Chen, Y., Li, Y., Lu, A., Yao, Y., Dai, J., Wang, Y., Liu, B., Lacey, S.D., Pastel, G.R., et al. (2017). Universal, *in situ* transformation of bulky compounds into nanoscale catalysts by high-temperature pulse. *Nano Lett.* 17, 5817–5822.
52. Voiry, D., Yang, J., Kupferberg, J., Fullon, R., Lee, C., Jeong, H.Y., Shin, H.S., and Chhowalla, M. (2016). High-quality graphene via microwave reduction of solution-exfoliated graphene oxide. *Science* 353, 1413–1416.
53. Fei, H., Dong, J., Wan, C., Zhao, Z., Xu, X., Lin, Z., Wang, Y., Liu, H., Zang, K., Luo, J., et al. (2018). Microwave-assisted rapid synthesis of graphene-supported single atomic metals. *Adv. Mater.* 30, 1802146.